AAS 19-035

EARLY NAVIGATION PERFORMANCE OF THE OSIRIS-REX APPROACH TO BENNU

Peter G. Antreasian*, Michael C. Moreau†, Coralie D. Adam*, Andrew French*, Jeroen Geeraert*, Kenneth M. Getzandanner†, Dolan E. Highsmith‡, Jason M. Leonard*, Erik Lessac-Chenen*, Andrew Levine*, Jim McAdams*, Leilah McCarthy*, Derek Nelson*, Brian Page*, John Pelgrift*, Samantha Rieger†, Eric Sahr*, Daniel Wibben*, Bobby Williams*, Kenneth Williams*, Dante Lauretta§, and the OSIRIS-REx Team.

The New Frontiers–class OSIRIS-REx (Origins, Spectral Interpretation, Resource Identification, Security–Regolith Explorer) mission is the first American endeavor to return a sample from an asteroid. In preparation for retrieving the sample, OSIRIS-REx is conducting a campaign of challenging proximity-operations maneuvers and scientific observations, bringing the spacecraft closer and closer to the surface of near-Earth asteroid (101955) Bennu. Ultimately, the spacecraft will enter a 900-meter-radius orbit about Bennu and conduct a series of reconnaissance flybys of candidate sample sites before being guided into contact with the surface for the Touch and Go sample collection event. Between August and December 2018, the OSIRIS-REx team acquired the first optical observations of Bennu and used them for navigation. We conducted a series of maneuvers with the main engine, Trajectory Correction Maneuver, and Attitude Control System thruster sets to slow the OSIRIS-REx approach to Bennu and achieve rendezvous on December 3, 2018. This paper describes the trajectory design, navigation conops, and key navigation results from the Approach phase of the OSIRIS-REx mission.

INTRODUCTION

The New Frontiers–class OSIRIS-REx (Origins, Spectral Interpretation, Resource Identification, Security–Regolith Explorer) mission will return a sample of near-Earth asteroid (101955) Bennu. This sample will provide insight into the initial states of planet formation and the origin of life. The data collected at the asteroid will also improve our understanding of asteroids that can impact Earth.[1,2] In preparation for retrieving a sample, OSIRIS-REx is conducting a campaign of challenging proximity operations maneuvers and scientific observations, bringing the spacecraft closer and closer to the surface. Ultimately, the spacecraft will enter a 900-meter-radius orbit about Bennu and conduct a series of reconnaissance flybys of candidate sample sites before being guided into contact with the surface for the Touch and Go (TAG) sample collection event.

The spacecraft's recent arrival at Bennu is the culmination of a two-year journey that commenced with launch from Cape Canaveral Air Force Station on September 8, 2016. The two-year cruise phase of the mission included an Earth gravity assist (EGA) in September 2017. The cruise

* KinetX, Inc., Space Navigation and Flight Dynamics (SNAFD) Practice, Simi Valley, CA, USA
† NASA/GSFC, Code 595, 8800 Greenbelt Road, Greenbelt, MD, USA.
‡ Aerospace Corporation, 14745 Lee Road, Chantilly, VA, USA
§ University of Arizona, Lunar and Planetary Laboratory, Tucson, AZ, USA

trajectory and some key mission activities during cruise are illustrated in Figure 1. We executed one Deep Space Maneuver (DSM-1) and three Trajectory Correction Maneuvers (TCM-1, TCM-2a, and TCM-3) during the first year of cruise to target the spacecraft to the B-plane geometry necessary for a successful Earth flyby. Antreasian *et al*.[3] discuss the navigation performance from launch through the EGA. After EGA, we executed DSM-2 on June 28, 2018, putting the spacecraft on track to reach the vicinity of Bennu in October 2018.

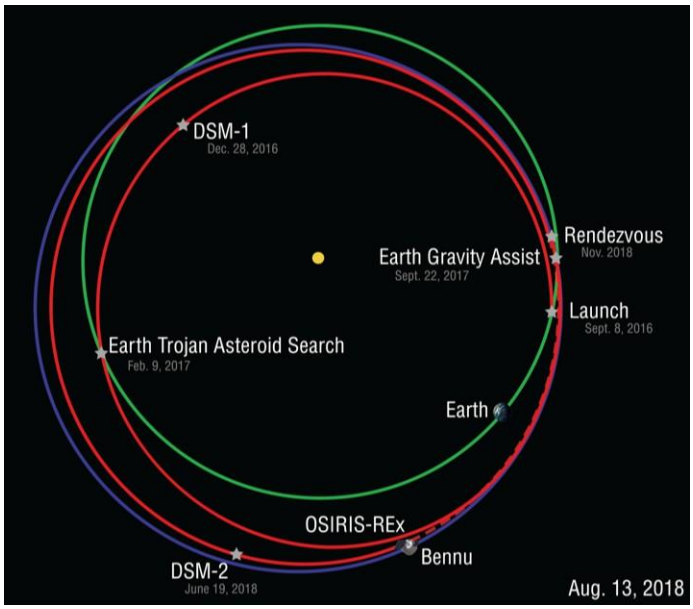

Figure 1: Trajectory and key mission events during OSIRIS-REx's two-year outbound cruise.

This paper summarizes some of the early navigation results and experiences from the Approach phase of the mission and the initial encounter with Bennu during the fall of 2018. On October 1, and again on October 15, we used the spacecraft main engine (ME) thrusters to slow the vehicle, and we commenced a weekly series of maneuvers designed to fly the spacecraft through a precise corridor to conduct early observations of Bennu, search its vicinity for dust plumes and natural satellites, collect images to characterize phase function and photometric properties, and conduct high-resolution imaging for the construction of an initial global shape model. The Approach phase of the mission concluded on December 3, 2018, when the spacecraft arrived at a location 18.6 km from Bennu and commenced a series of close flybys called the Preliminary Survey. The schedule of activities for the first three phases of the mission is illustrated in Figure 2.

We provide a detailed summary of the different optical navigation (OpNav) techniques employed as Bennu transitioned from a point source to a resolved object. We compare performance across the spacecraft's different imagers, with results from both unresolved and resolved body centerfinding. We summarize the orbit determination (OD) performance during the late cruise and early Approach phase, including how pre-launch estimates of predictive uncertainties compare to actual performance. We include a summary of the performance of the propulsive maneuvers conducted during this period, namely, a series of six maneuvers spanning the ME, TCM, and Attitude Control System (ACS) thruster sets. The largest of these maneuvers involved a change in velocity of more than 351 m/s, whereas the smallest was just over 1 cm/s.

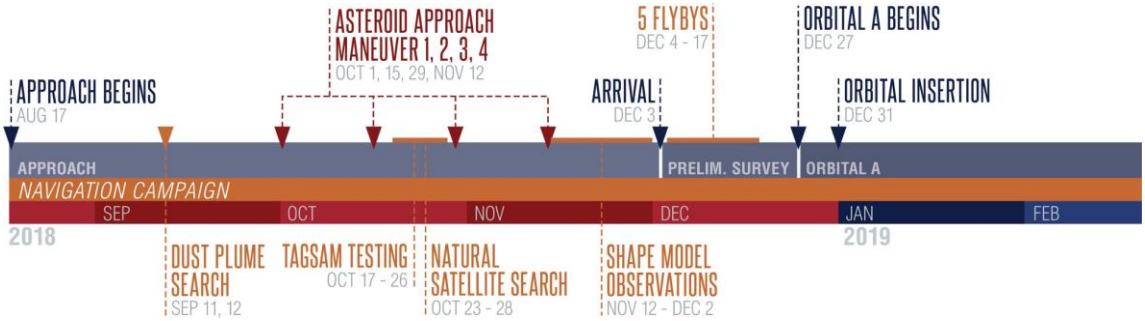

Figure 2: Schedule and activities for the Approach, Preliminary Survey, and Orbit A mission phases.

APPROACH TRAJECTORY DESIGN

The OSIRIS-REx Approach trajectory was designed to create a robust, gradual approach to Bennu, to optimize initial characterization of the asteroid and its surrounding dynamical environment, and to slow the spacecraft velocity relative to Bennu by the beginning of proximity operations. Each science objective during this phase placed different requirements on the trajectory, which defined a corridor through which the spacecraft must fly.[2] For example, lightcurve and phase function measurements required the spacecraft to traverse a large range of phase angles (also known as Sun-asteroid-probe angles), whereas the spectrometry and natural satellite imagery were best performed at very low phase angles. Finally, the shape model imaging needed to take place near the end of Approach when the spacecraft was close to Bennu to achieve the desired resolution, but it also had to be done at several different phase angles and lighting conditions.

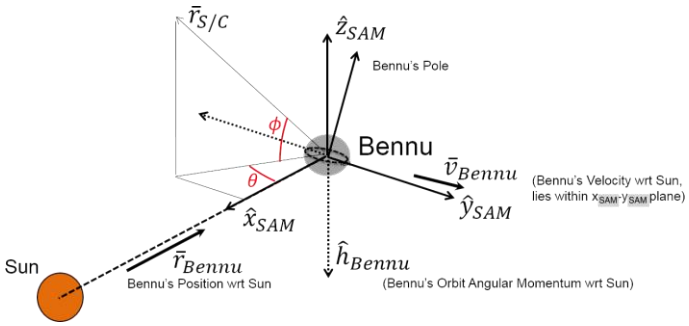

Figure 3: OSIRIS-REx Sun Anti-Momentum (SAM) coordinate frame definition.

We targeted the final Approach trajectory to Bennu with the EGA in September 2017, which changed the spacecraft outbound cruise trajectory to match the orbit inclination of Bennu, and the 16.6 m/s DSM-2 burn on June 28, 2018, which targeted a location 6500 km from Bennu on October 5, 2018. To satisfy the science requirements and slow the spacecraft's approach velocity from its heliocentric trajectory, the Approach phase contained four deterministic Asteroid Approach Maneuvers (AAMs): AAM-1 through AAM-4. The first two maneuvers of the sequence were designed to provide a single set of arrival conditions for all launch opportunities that were compatible with the spacecraft operational design; they are among the largest to be performed during the mission and were critical to slowing down the spacecraft's Bennu-relative velocity from nearly 500 m/s to ~5 m/s. In addition, the sequence was designed to enable graceful recovery if AAM-1 was not executed successfully. AAM-2 placed the spacecraft at 250 km from Bennu and near zero degrees phase angle in support of science observations. AAM-3 targeted specific illumination conditions in support of the shape model imaging and further slowed the spacecraft's Bennu-relative velocity to ~0.1 m/s. The final maneuver of the sequence, AAM-4, targeted the Bennu B-plane

conditions necessary for the start of the Preliminary Survey phase, which marked the official arrival at Bennu and beginning of proximity operations.

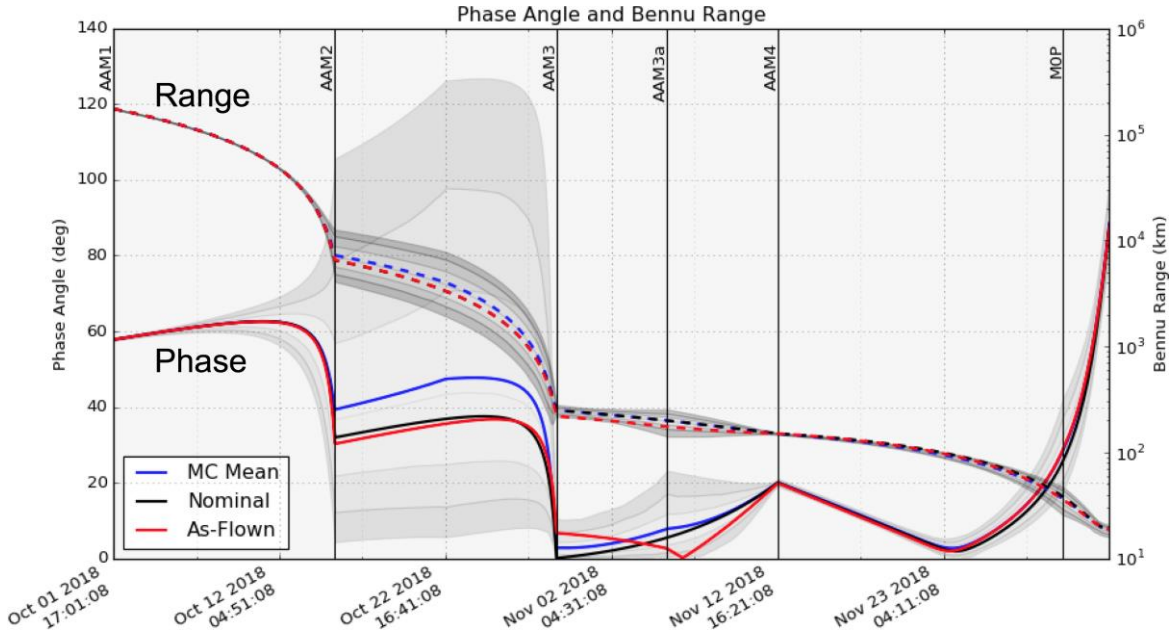

Figure 4: Nominal Approach range and phase angle profile (black), compared to pre-encounter Monte Carlo mean (in blue) and the as-flown profile (red). Solid lines indicate solar phase angle; dotted lines are the range to Bennu. Grayscale variations depict 1-, 2-, and 3-sigma Monte Carlo dispersions.

At this early stage of the mission, we did not yet know Bennu's shape, orientation, and surface geometry; thus, it was vital that the mission use a consistent Bennu-centric coordinate frame that is independent of these features to design and analyze the incoming trajectory. The selected coordinate frame, named the Sun Anti-Momentum (SAM) frame, is defined solely based on Bennu's orbit, as depicted in Figure 3. This coordinate system has its origin at Bennu's center of mass. The *x*-axis points along the Bennu-Sun line, the *z*-axis is in the opposite direction of Bennu's heliocentric orbital angular momentum vector, and the *y*-axis completes the right-handed frame. Representing the spacecraft position in this frame in spherical coordinates defines the values of solar longitude and solar latitude (θ and φ in Figure 3, respectively) that we used as a reference for maneuver targets and science observation constraints during this phase.

The nominal approach trajectory profile placed the spacecraft across a wide variety of solar latitudes and longitudes to satisfy the science observation constraints. The nominal trajectory profile in terms of Bennu range and phase angle is shown in Figure 4. The observing constraints for science posed an early challenge for navigation because they required precise delivery of the spacecraft while it was still several hundreds of kilometers away from the asteroid. These requirements, along with the relatively large size of the early AAMs, led to the introduction of statistical cleanup maneuvers AAM-2a and AAM-3a into the nominal schedule to better control the approach trajectory of the spacecraft. We also scheduled a small statistical maneuver, M0P, to clean the propagation of errors from AAM-4 and potential OD prediction errors that could accumulate over the last two weeks of Approach. This maneuver ensured the precise arrival at the M1P maneuver location on December 3 for the initiation of Preliminary Survey. The overall schedule of all of the Approach maneuvers, and their nominal locations in the Bennu-centered SAM coordinate frame, are listed in Table 1. Because each maneuver is placed at a key location in this trajectory to satisfy requirements, the targeting strategy for each maneuver is to achieve the location

of the next maneuver of the sequence; e.g., AAM-1 was executed to target arrival of the spacecraft at the AAM-2 location.

Table 1: OSIRIS-REx Approach maneuver schedule and nominal Bennu-relative locations.

Event	Date (UTC)	Range (km)	Solar Latitude (deg)	Solar Longitude (deg)	Pre-Burn Velocity (m/s)	Phase (deg)
DSM-2	Jun 28, 14:30	5,580,000	N/A	N/A	–	N/A
AAM-1	Oct 1, 17:00	175,000	20.5	55.3	491.3	58.0
AAM-2	Oct 15, 17:00	6,500	0.0	32.0	141	32.0
AAM-2a	Oct 22, 17:00	3,325	0.0	36.8	5.2	36.8
AAM-3	Oct 29, 17:00	250	0.0	0.0	5.2	0.0
AAM-3a	Nov 5, 17:00	200	0.0	-5.5	0.12	5.5
AAM-4	Nov 12, 17:00	150	0.0	-20.0	0.15	20.0
M0P	Nov 30, 17:00	38.3	8.7	24.2	0.12	25.6
Bennu Arrival*	Dec 3, 17:00	18.6	22.3	89.6	0.14	89.6

*Time of M1P maneuver that begins Preliminary Survey

OPTICAL NAVIGATION PERFORMANCE AND RESULTS

The first image of Bennu was recorded with OSIRIS-REx's PolyCam high-resolution imager[4] on August 17, 2018, when the spacecraft-to-asteroid range was ~2,184,000 km. We used star-based optical navigation for the entire duration of Approach owing to the necessity to estimate body-relative states before adequate digital terrain maps are available for landmark-based OpNav. We used the KinetX KXIMP software suite to produce star-based OpNav observables throughout the duration of Approach.

PolyCam and the MapCam medium-field imager[4] acquired the baseline OpNav images during the Approach phase. Additionally, the wide field-of-view (FOV) NavCam imager acquired test images to help inform exposure times and uncover potential unknown issues before relying on NavCam[5] as the prime OpNav instrument after December 2. The PolyCam, MapCam, and NavCam optical and radiometric specifications are presented in Table 2. The layout of the three imagers on the spacecraft instrument deck is shown in Figure 5. From August 17 through November 12 (AAM-4), 2018, PolyCam was the prime OpNav instrument, with the exception of October 16–17 and October 30–31, when we used MapCam to guarantee capture of the asteroid in a single frame given burn execution errors. Starting on November 13, MapCam became the prime OpNav imager for the remainder of Approach.

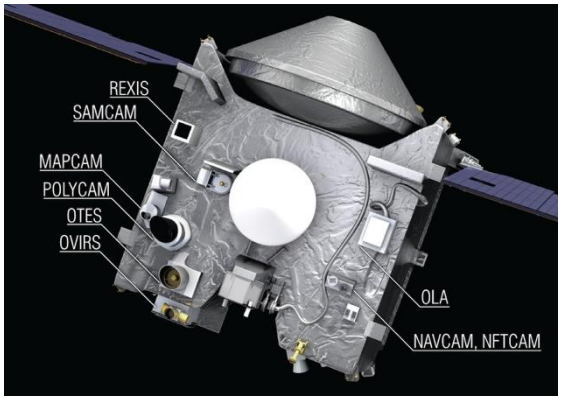

Figure 5: Illustration of the spacecraft instrument deck indicating the layout of primary instruments (credit: Heather Roper/University of Arizona).

Table 2: OpNav imager optical and radiometric properties.

	PolyCam (at ∞)	MapCam (PAN)	NavCams 1 & 2
FOV (°)	0.8 x 0.8	4 x 4	44 x 32
iFOV (μrad/px)	13.5	68	280
Detector size (px)	1024x1024	1024x1024	2592x1944
Aperture (mm)	175	38	2.28
F/#	3.5	3.3	3.5
Focal length (mm)	630	125	7.6
Pixel size (microns)	8.5x8.5	8.5x8.5	2.2x2.2

Once Bennu became bright enough to reach the saturation limit of the detector in a 4-second image (September 26, 2018), the imaging scheme began alternating between short and long exposures. We used the short exposures to acquire a well-exposed image of Bennu and the long exposures to image background stars within the FOV and calculate the inertial attitude of the images.

From a navigation perspective, the Approach phase can be split into two regimes: early Approach, when Bennu was treated as an unresolved target, and late Approach, when Bennu was treated as a resolved target. Bennu transitioned from an unresolved to a resolved target in the PolyCam imager on October 18, 2018. We present the OpNav techniques and results for these two paradigms.

Early Approach Phase: Unresolved Centerfinding

The early Approach phase spanned from August 17 through October 17, 2018. The imaging cadence started at three OpNav observation sets per week until October 2, 2018, when it increased to a daily cadence after AAM-1. Four-second exposures were sufficient for stellar imaging. This exposure time was also sufficient for imaging Bennu until September 26 (400,000 km range), when the asteroid's apparent magnitude could cause over-exposure. From that day forward, exposures alternated between 4-second stellar images and shorter asteroid-tuned exposures, which stepped down from 2 seconds to 4 milliseconds during early Approach.

Point-Source Centerfinding Techniques

We used point-source centroiding algorithms to calculate the centroids of objects that are ~3 pixels in diameter or less. We fit a 2D Gaussian function to the point-source image data in a least squares sense to determine the best estimate for the centroid. We used this method on both stars and unresolved targets. When the apparent diameter of the target subtends a substantial portion of the pixel, we had to account for a phase effect to correct the observed center of brightness (COB) to the desired center of figure (COF). We determined the correction by rendering the target in a sub-sampled simulation and computing the difference between the observed COB and the known COF. We then applied this offset to the real image centroid (COB) to obtain the COF navigation observable.

Results and Performance

The post-fit centerfinding residuals for the unresolved, early Approach Phase are shown in Figure 6; the top plot is the raw sample and line centroid residuals, and the bottom is converted to physical units based on image resolution. We computed the residual by differencing the predicted centroid, based on the reconstructed trajectory, from the observed centroid. In the early data set, we observed a small bias in the line measurement due to PolyCam and MapCam detector aliasing at low signals. Once the Bennu signal level crossed an empirically derived threshold around September 17, we expected that the measurements would no longer be biased. This date is

consistent with the OD post-fit residual trends in Figure 6.

The centerfinding accuracy requirements for navigation with Bennu as a point source are 1 pixel, 1-sigma. The statistics on these post-fit residuals suggest accuracies nearly an order of magnitude better than the requirement, at around 0.1 pixel, 1-sigma.

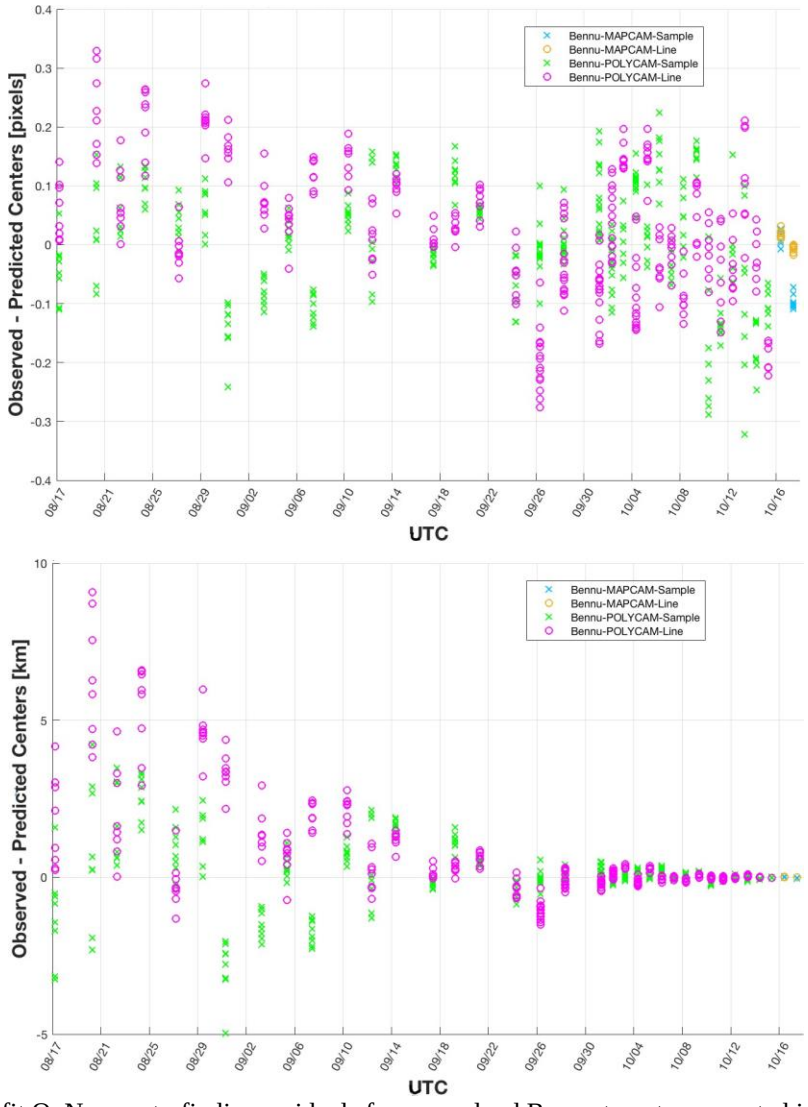

Figure 6: Post-fit OpNav centerfinding residuals for unresolved Bennu targets, presented in camera frame (top) and physical space (bottom).

Late Approach Phase: Resolved Centerfinding

Bennu subtended 7 pixels in the PolyCam instrument when it became a resolved target on October 18. By the last day of PolyCam OpNav imaging on November 12, at ~250-km range, the apparent diameter had grown to nearly 250 pixels. When we switched to the wider-FOV (4-degree) MapCam as the prime imager, the apparent diameter of the body varied from 50 pixels on November 13 to 300 pixels on December 2.

Extended-body Centerfinding Techniques

We used extended-body centroiding algorithms to calculate centroids of targets that are greater than 3 to 5 pixels. KXIMP contains a suite of algorithms and modeling capabilities for finding the centroid of an extended target.[6,7] The primary method used during Approach was 2D cross-correlation, which uses the predicted size, position, and rotation state of the target. It performs a ray-tracing process to simulate a best estimate of the target image. This simulated image is then cross-correlated with the flight image data to produce an estimate for the target centroid. There are many options for tuning how the asteroid is rendered in the simulated image—namely the shape model, albedo maps, spin state, and surface reflectance properties. Estimating formal uncertainty is challenging for extended-body centroiding. To give the analyst a visual reference as to how well the algorithm calculated the centroid, plots are produced showing the real data, simulated data, post-fit difference between real and simulated data, and a summary image with the centroid and shape model limb overlay. Examples are shown below.

Another technique available in the KXIMP suite is limb-scanning, which can be used to estimate relative scale (range or shape scale error).[8] We used this method during Approach as a spot-check on the cross-correlation algorithm. The comparison provided confidence in the baseline centroid solutions, and we observed no substantive relative scale.

Results and Performance

The *a-priori* shape model of Bennu was derived from Arecibo Radar Telescope data by Nolan *et al*.[9] We used this shape as the baseline in the OpNav centerfinding algorithms for the first few weeks of extended-body centerfinding, from October 18 through November 9, 2018. On October 22, the mission adopted a refinement to the asteroid spin state. To render a simulated image of the model, a surface reflectance law must be assumed. We assumed the nominal Lommel-Seeliger scatter law from the Design Reference Asteroid mission document as the *a-priori* bi-directional reflectance distribution function.[10,11] On November 9, the mission adopted a new shape model and spin state (hereafter, the 11/9 shape model).[12]

Figure 7 shows results from the 2013 radar shape model compared with a PolyCam image taken on October 29, 2018. The left graphic shows the simulated image used in the cross-correlation, in a false color map scaled by signal data number. The center graphic is the result from differencing the real and simulated image, aligned based on the computed centroid solution. Finally, the graphic on the right shows the real image of Bennu, with the observed centroid solution marked by a blue cross and an outline of the shape model overlaid in white. Although the *a-priori* model was exceptionally close to the real shape and provided sufficient centroid solutions leading up to AAM-3a, deviations were visible as Bennu's true shape was revealed at ever-increasing resolution.

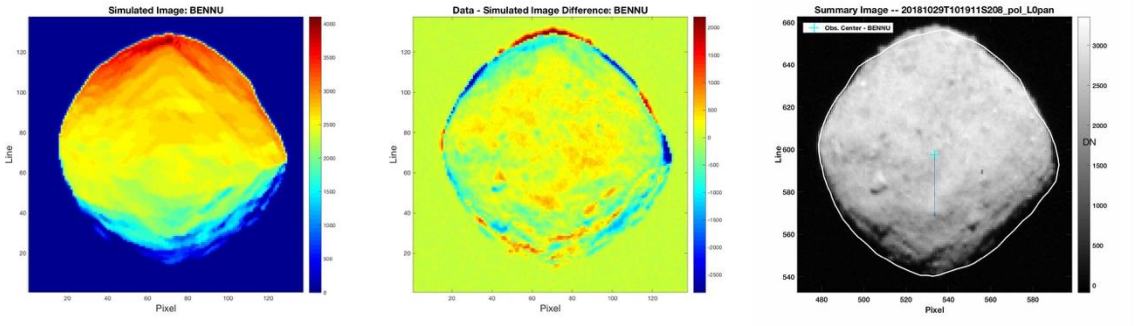

Figure 7: Left: Simulated image of Bennu at the epoch and geometry of the Oct. 29 PolyCam OpNav, using the 2013 radar shape model. Center: Difference between the real and simulated images. Right: Nov. 29 PolyCam OpNav image with the observed center (blue cross) and shape model outline (white) overlaid.

The 11/9 shape model and spin state demonstrated improved modeling and centroiding over the *a-priori* radar model. Figure 8 shows the 11/9 shape model performance on the same October 29 PolyCam image as shown in Figure 7. We used the 11/9 shape model to re-process OpNav data back to October 15, and it held up well as the baseline model through the final week of the Approach phase. Figure 9 shows that the difference in the centroid solutions between the *a-priori* and 11/9 shape models are within 1.5 pixels. When converting to physical space (bottom plot), the 1-sigma errors are on the order of 3 m in the instrument sample direction and 2.5 m in the line direction. In the absence of trustworthy formal errors, we evaluate these differences to help bound the centerfinding error. To assess OpNav measurement errors against the OD requirements and weighting assumptions, we convert these errors to percentage of apparent body diameter. The errors are ~0.5%, 1-sigma, which is more than a factor of 2 better than the requirement of 1 pixel + 1% of the body diameter, 1-sigma, assumed in the OD as shown by Equation 1.

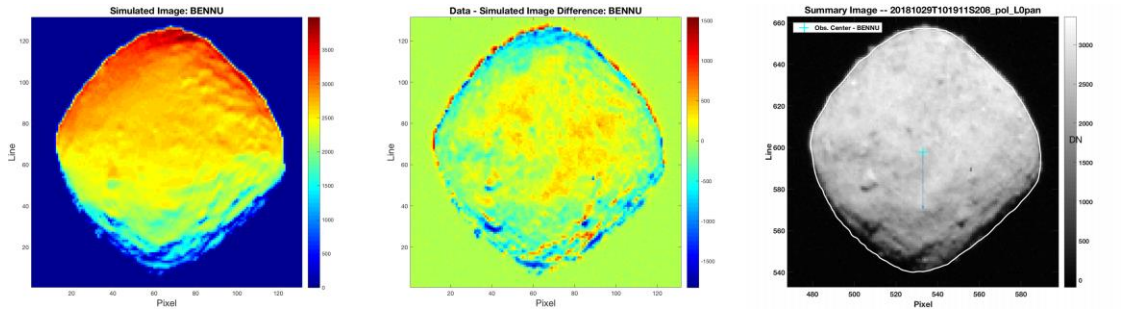

Figure 8: Left: Simulated image of Bennu at the epoch and geometry of the October 29 PolyCam OpNav using the 11/9 shape model. Center: Difference between the real and simulated images. Right: November 29 PolyCam OpNav image with the observed center (blue cross) and shape model outline (white) overlaid.

The post-fit residuals from the 11/9 shape model are shown in Figure 10. The results show residuals less than 1 pixel, with standard deviations on the order of 0.1 to 0.3 pixels. In physical space, we observe residuals less than 10 m, with standard deviations on the order of 1 to 3 m or 0.2 to 0.6% of the body diameter. After AAM-3 on October 29, the residuals are bounded within +/- 3 meters. Comparing this to the requirements for OD, we observe the OpNav centerfinding performance to be as much as an order of magnitude better than requirements. This performance can be attributed to excellent *a-priori* and early in-situ shape model development.

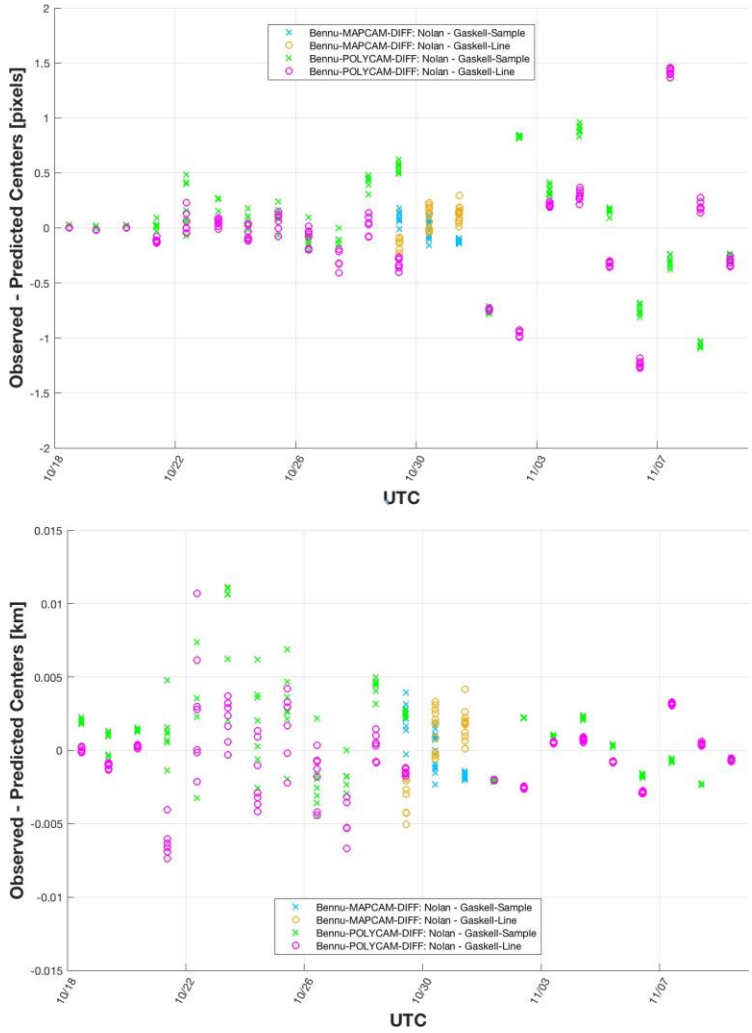

Figure 9: Differences between the 2013 radar shape model (Nolan) and the 11/9 shape model (Gaskell) OpNav centroid solutions, presented in camera frame (top) and physical space (bottom).

ORBIT DETERMINATION RESULTS AND EXPERIENCES

The purpose of OD is to reconstruct and predict the spacecraft trajectory. OD uses radiometric tracking data and optical images from Approach to minimize the difference between the computed and observed measurements and estimate the spacecraft state (position and velocity), as well as other parameters governing the dynamics and measurements of the system.

During the latter portion of the outbound cruise and Approach, we refined the modeling of the spacecraft to produce better-quality predictions. The Solar Radiation Pressure (SRP) model is the 10-plate model developed for OSIRIS-REx.[13] We updated the reflectivity coefficients based on data from the outbound cruise and Approach. In addition, we removed the re-radiation portion of the diffuse coefficient and developed a detailed thermal re-radiation model for the spacecraft based on the temperature profile of the spacecraft surfaces at various illuminating conditions over multiple distances from the Sun. We used phase-center offsets for each antenna to better model spacecraft slews and antenna offsets in ranging passes. During cruise, we noticed that the internal path delays of the telecom system were in error. Multiple passes for which an antenna change occurred mid-pass indicated a bias between the low-gain (LGA), medium-gain (MGA), and high-gain (HGA) antennas. We estimated per-antenna internal path delays for the LGA and MGA relative

to the HGA (+X LGA, –X LGA, and –X MGA) and updated them for Approach. All of these updates to the modeling allowed the trajectory reconstructions and predictions to outperform the anticipated errors determined in covariance studies.

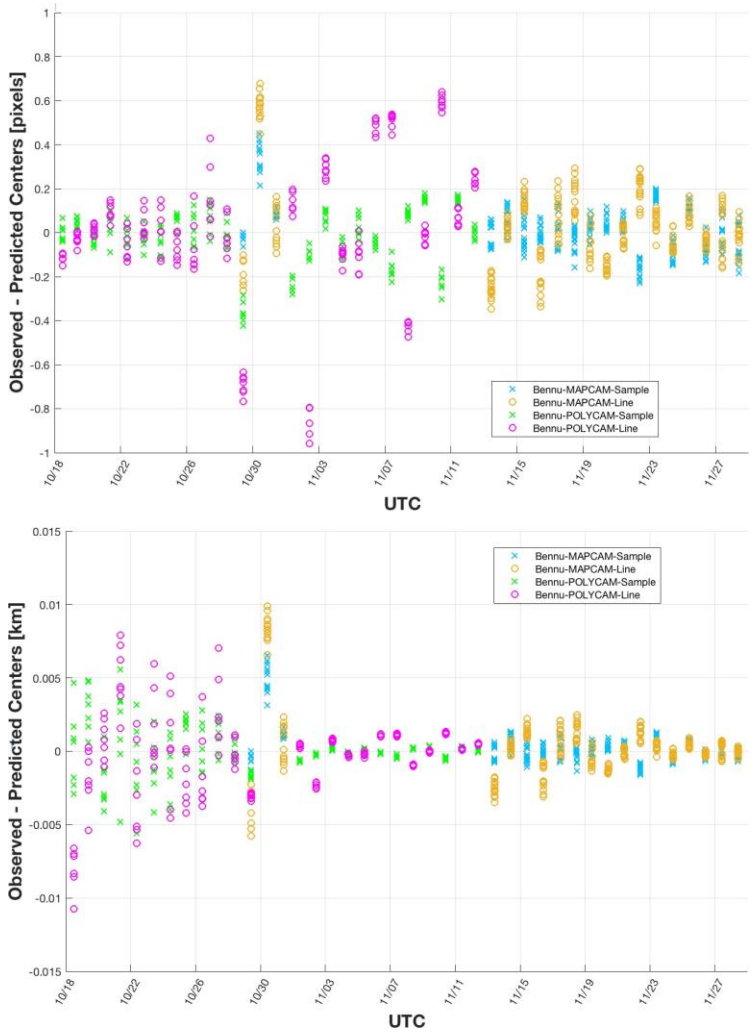

Figure 10: Post-fit OpNav centerfinding residuals for resolved Bennu targets using the 11/9 shape model, presented in camera frame (top) and physical space (bottom).

Approach OD Schedule

Throughout Approach, there were various users of the OD products, including the teams responsible for spacecraft navigation and operations, the Deep Space Network, and the mission science teams. We developed a schedule for Approach to provide reconstructed and predicted ephemeris solutions to each of these teams based on predicted performance of the trajectory errors provided in covariance analysis.

OpNav and maneuver design require predicted trajectories and their associated uncertainties. We developed OD delivery date requirements for OpNav based on predicted covariance analysis uncertainties to determine the necessary imager and resolutions, as well as any potential for scanning. We scheduled onboard ephemeris updates for the purpose of maintaining Bennu in the FOV of the desired imager. Approach was the first time in the mission that ephemeris late updates occurred. This type of update involves downlinking the current day's worth of OpNav images and

radiometric tracking data and producing a trajectory estimate that is turned around within 24 hours to uplink to the spacecraft for nadir-relative pointing updates onboard. Trajectory solutions were typically provided 14 days in advance for the preliminary maneuver design phase during Approach and 5 to 7 days in advance for the final maneuver design phase. For the majority of proximity operations, we use maneuver late updates (or 24-hour turnarounds in the maneuver design). The cleanup maneuver, M0P, at the end of Approach was the first maneuver to test this quick-turnaround activity, albeit over 48 hours instead of 24 for a typical late update.

Filter Strategies

Approach provided the opportunity to begin processing centerfinding OpNav measurements of Bennu for the first time. Centerfinding test images of Earth and the Moon obtained during the EGA,[14] and of Jupiter shuttered during the Earth-Trojan asteroid search (February 2017),[15] allowed us to assess the ingestion of centerfinding OpNavs before Approach and indicated expected levels of performance from the imagers and OD process. Testing during the outbound cruise provided opportunities to update the filter strategy for Approach.[16] The operations navigation filter setup was derived from the lessons learned in these activities and other operational readiness tests. We maintained a baseline filter strategy throughout Approach, with slight refinements depending on what was being estimated. In addition to the baseline filter strategy, we used multiple filter cases or variations as a check to the baseline setup. Variations occur in the estimated parameters and associated uncertainties, in different measurement combinations and weighting schemes, and in the level of stochastic acceleration error. We compared these estimated trajectory solutions to determine the consistency between the reconstructed and predicted states, variations in the non-dynamic bias parameter estimates, and the contribution of consider covariance inflation to estimated parameters. Below is an example of our baseline filter strategy.

<u>Filter Estimated Parameters</u>

- Spacecraft epoch state
- SRP scale factor
- 3-axis momentum desaturations (desats) at 2.0 mm/sec (7-day campaign) and 0.5 mm/sec (3-day campaign after AAM-3, October 29, 2018)
- RA, DEC, Force of finite burns
- Bennu ephemeris (SETIII Parameters[17])
- 3-axis stochastic acceleration (3e-12 km/s^2) to account for small forces (spacecraft IR, asteroid IR, albedo, SRP)
- Per-pass range biases

<u>Consider Parameters</u>

- DSN station locations (correlated cov, from 2016 survey)
- Earth ephemeris (SETIII Parameters[17]) (correlated covariance, from DE430[18])
- Media errors (Ionosphere Day, Night, Troposphere Wet, Dry)
- Polar motion, UT1 errors
- Future desats

<u>X-Band Radiometric Tracking</u>

- 2-way Doppler (weighted at 3x the RMS per pass)
- 2-way Range (weighted at 3x the RMS per pass)
- DDOR (weighted at 0.06 nanoseconds)

<u>Centerfinding OpNavs</u>

- Early Approach (August 17–September 30), 3 image sets every week
- Mid Approach (October 1–November 29), 1 image set every day

- Late Approach (November 30–December 3), 3–8 image sets per day
- PolyCam (prime imager: August 17–November 12)
- MapCam (AAM-2 + 2 days (October 16–17), AAM-3 + 2 days (October 30–31), prime imager: November 13–December 3))
- NavCam (test images: October 30–December 3; prime imager: after December 3)

Radiometric data are typically weighted at the standard deviation of the noise level computed from the residuals on a per-pass basis scaled by 3 times. The weights applied for the centerfinding OpNavs are determined by

$$W = (W^2_{\text{min}} + (C * d)^2)^{1/2} \quad (1)$$

where W_{min} is the minimum weight (1.0 pixel), C is the apparent diameter scale factor (1% of the diameter), and d is the apparent diameter of the asteroid in pixels. The apparent diameter of the asteroid in pixels can be computed by

$$d = da/(r * iFOV) \quad (2)$$

where d_a is the diameter of the asteroid (nominally 512 m for Bennu), r is the range to the asteroid surface, and $iFOV$ is the angular resolution of the detector (rad/pix).

Bennu Ephemeris Estimation

The *a-priori* ephemeris for Bennu was estimated by the Solar System Dynamics Group at NASA's Jet Propulsion Laboratory (JPL) as solution number 76.[19] JPL's solution 76 was based on 478 ground-based right ascension (RA) and declination (DEC) observations of Bennu, as well as 22 radar delay and seven Doppler measurements from the Arecibo and Goldstone radars in 1999, 2005, and 2011. At the time of Approach, the *a-priori* Bennu ephemeris position uncertainty (1-sigma) based on solution 76 was about 12 km or 0.4 pixels in the PolyCam imager. Centerfinding OpNavs on August 17, 2018, detected Bennu ~0.7 pixels (20 km) off of the *a-priori* position predicted by solution 76. From the start of Approach imaging on August 17, we estimated Bennu's ephemeris with each OpNav delivery using centerfinding OpNav techniques previously described. Figure 11 shows the estimated position and 3-sigma uncertainties of Bennu relative to the OSIRIS-REx spacecraft in ICRF RA and DEC over the course of Approach, mapped to the start of Approach imaging on August 17, 2018. We quickly converged on the Bennu ephemeris and refined its estimates over the course of Approach.

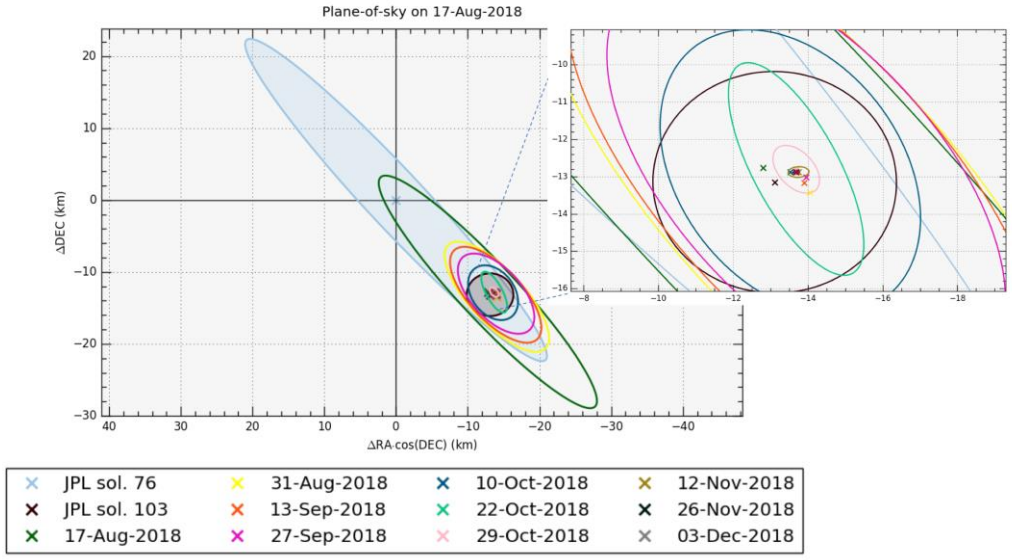

Figure 11: Estimated Bennu ephemeris and error ellipses (3-sigma) as seen from the OSIRIS-REx plane of sky on August 17, 2018.

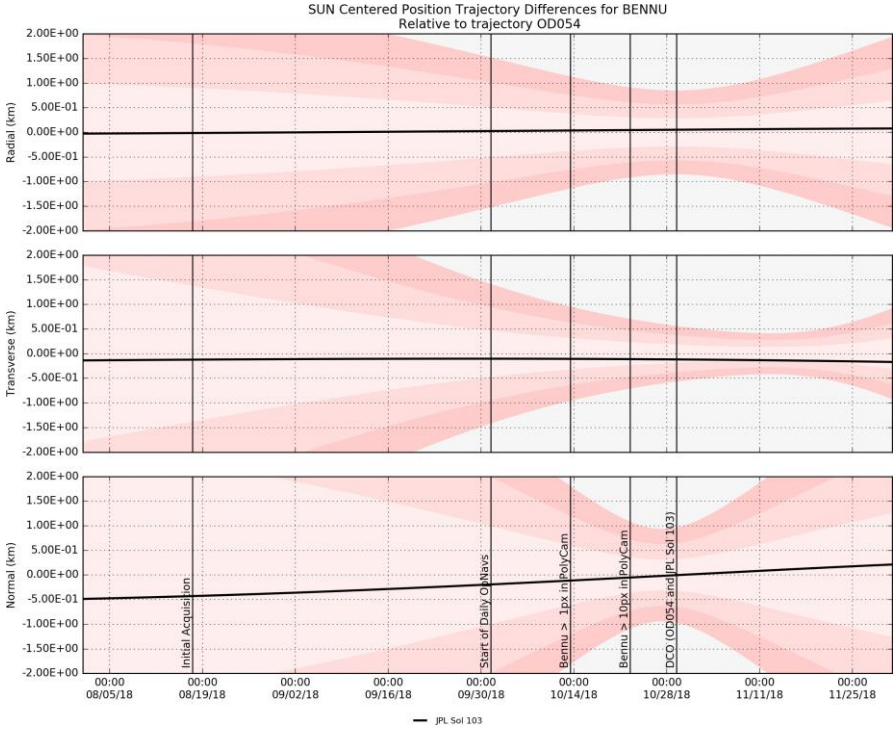

Figure 12: Estimated Bennu Sun-centered radial-transverse-normal trajectory differences and uncertainties.

In November 2018, JPL delivered an updated solution to Bennu's ephemeris, solution 103.[20] Solution 103 included the same ground-based observations as solution 76 but also incorporated images of Bennu through October 29. Solution 103 matched the ephemeris estimate that we determined to well within 1-sigma of the latter's formal uncertainties. Figure 12 compares the solution 103 ephemeris with our estimated Bennu ephemeris and uncertainty with a data cutoff (DCO) of October 29, 2018.

Orbit Determination Prediction Performance

Throughout Approach, we updated the onboard ephemeris to maintain a certain precision in Bennu nadir-relative targeting to capture OpNav images and achieve specific science targets. Early phase analysis determined a timeline of when the onboard ephemeris would need to be updated for OpNavs to reduce the likelihood of Bennu being clipped in the images or even missing from the FOV. We developed a set of uncertainties for associated DCOs based on the predicted performance and uncertainties assumed at the time, governing both the spacecraft dynamics and the unknown Bennu small-body environment.[21]

We evaluate the predicted errors for Approach by comparing the deviation in the predicted trajectory to the reconstructed trajectory then normalizing by the predicted uncertainties. Figure 13 shows the number of sigma variations of each of the predicted trajectories that went onboard compared to the latest reconstructed trajectory. In general, the onboard predicted errors are less than 1-sigma. Figure 13 contains post-maneuver radio data–only reconstructs. These updates typically produce the largest errors immediately after the burn owing to the inability of a few hours of Doppler data to fully constrain the solution. However, these radio-only trajectories were put onboard to limit the pointing errors for imaging sequences taken immediately after the burn. After AAM-4, the OD prediction errors remained remarkably low, with variations of less than 0.5-sigma, producing predicted OpNav errors of only a few pixels. Figure 14 compares the OD solutions delivered after AAM-4 to the AAM-4 target in the Bennu-centric Bennu-equatorial B-plane mapped to the time of closest approach on December 3, 2018 (18:30 UTC). This mapping time is convenient for evaluating performance, but the closest approach was never achieved because the M1P maneuver executed 1.5 hours beforehand to begin the Preliminary Survey phase. The concentric OD solutions, OD061–66, over the two-week span of November 14–28 in Figure 14 verify the predictive performance of the spacecraft small-force modeling. The predicted trajectory errors of these solutions were generally less than 500 m propagated over two weeks. This finding indicates that we modeled the small forces to better than 1.0×10^{-12} km/s^2. Figure 14 also shows that the AAM-4 target was finally achieved after the1.4 cm/s M0P maneuver performance on November 30 was reconstructed in the post-M0P OD solutions, OD067–68. The 1-sigma uncertainties associated with the OD066 solution used for the M0P late-update design were about 62 m x 45 m in the B-plane and 650 sec in the time of closest approach. These uncertainties were reduced to, respectively, 52 m x 8 m and 130 sec in the last Approach-phase OD, OD068, which we used to design the first Preliminary Survey maneuver, M1P.

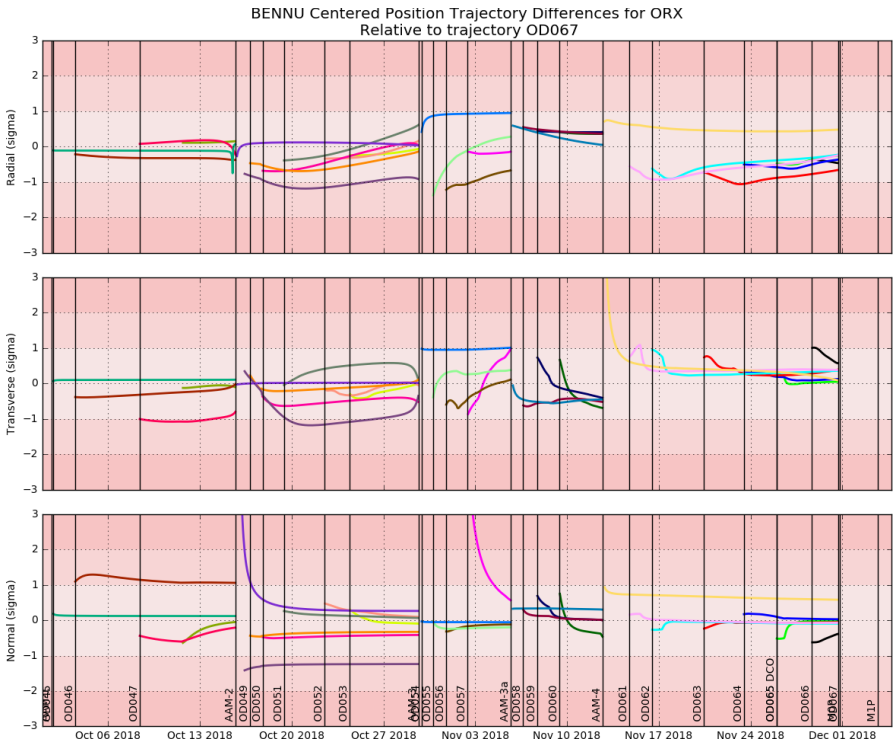

Figure 13: OSIRIS-REx prediction errors compared to the latest reconstructed Approach trajectory, normalized by the predicted uncertainty after the DCO.

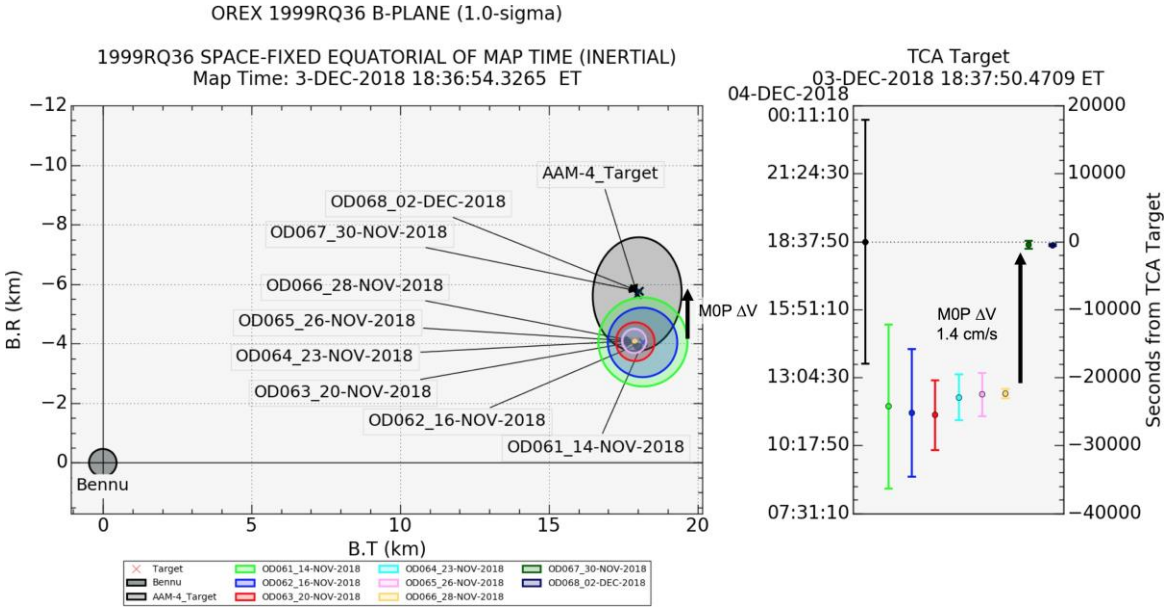

Figure 14: Post-AAM-4 OD solutions mapped to the time of closest approach on December 3, 2018, in the Bennu-centric Bennu-equatorial frame. TCA, Time of Closest Approach.

Table 3: OSIRIS-REx Approach maneuver execution performance.

Maneuver	Engine Type	Parameter	Nominal Value	Estimated Value	*A-priori* Sigma	Estimated Sigma	Correction	Correction / *A-priori*
DSM-2	TCM	ΔV (m/s)	16.6260	16.6302	0.0555	0.0014	0.0042	0.0758
		RA (deg)	99.8860	99.9111	0.2551	0.0081	0.0251	0.0984
		Dec (deg)	-46.1600	-46.2090	0.1767	0.0074	-0.0490	-0.2772
AAM-1 †	ME	ΔV (m/s)	351.2984	351.2821	1.1639	-0.0163	-0.0140	-0.7160
		RA (deg)	85.4970	85.52185	0.3382	0.0004	0.0249	0.0735
		Dec (deg)	8.1970	8.1692	0.3347	0.0004	-0.0278	-0.0831
AAM-2 †	ME	ΔV (m/s)	137.0493	137.0702	0.4486	0.0003	0.0209	0.0467
		RA (deg)	83.4480	83.4352	0.3400	0.0004	-0.0128	-0.0376
		Dec (deg)	7.5910	7.5912	0.3370	0.0004	0.0002	0.0005
AAM-3 ‡	TCM	ΔV (m/s)	5.1274	5.1428	0.1358	0.0002	0.0154	0.1133
		RA (deg)	124.6775	124.4032	0.6769	0.0062	-0.2743	-0.4052
		Dec (deg)	23.3612	23.4741	0.6630	0.0054	0.1129	0.1704
AAM-3a	ACS	ΔV (m/s)	0.0598	0.0602	0.0002	0.0003	0.0004	1.8568
		RA (deg)	230.2059	230.1800	0.3361	0.2452	-0.0259	-0.0771
		Dec (deg)	-29.8102	-29.8977	0.2916	0.2924	-0.0875	-0.3001
AAM-4	ACS	ΔV (m/s)	0.1698	0.1704	0.0005	0.0001	0.0005	1.0914
		RA (deg)	101.9920	101.8900	0.3277	0.1940	-0.1020	-0.3112
		Dec (deg)	27.1360	27.4226	0.2916	0.1277	0.2866	0.9827
M0P ‡	ACS	ΔV (m/s)	0.0133	0.0138	0.0004	0.0001	0.0005	1.2220
		RA (deg)	-176.0204	-175.5518	2.2873	0.2427	0.4687	0.2049
		Dec (deg)	-32.2113	-32.3421	1.0879	0.2307	-0.1308	-0.1202

† ME maneuvers included a 30-sec settling burn (2.1 m/s for AAM-1, 2.5 m/s for AAM-2)

‡ Total of maneuver decomposed into two components to avoid Sun Keepout Zone constraints

MANEUVER PERFORMANCE

A comparison of the as-flown trajectory against the nominal reference trajectory was shown in Figure 4. No contingency scenarios were required because all Approach maneuvers executed within expected errors. In fact, AAM-1 and AAM-2 performed so well that AAM-2a was waived off, as the change in velocity (ΔV) required to perform the maneuver was below the cutoff threshold. Even without AAM-2a, the delivery of the spacecraft to the AAM-3 location was within the expected 1-sigma trajectory dispersions based on Monte Carlo analysis; however, the decision to waive off the AAM-2a cleanup contributed to the AAM-3 design being such that it violated a spacecraft constraint related to pointing the instrument deck too close to the Sun. We therefore decomposed the maneuver design into two separate, Sun-safe segments that provided a resultant ΔV equivalent to the original design at the cost of a slight ΔV penalty. Although this process had been tested extensively, this was the first maneuver to be decomposed in-flight. The final design resulted in a cumulative ΔV of 5.22 m/s, with an effective ΔV of 5.13 m/s owing to the decomposition. After execution of these segments, trajectory dispersions were such that the AAM-3a maneuver was necessary to correct the course of the spacecraft ahead of AAM-4. On November 30, a small 1.4 cm/s decomposed maneuver, M0P, cleaned up trajectory dispersion from AAM-4.

A summary of the designed maneuver parameters and the reconstructed execution errors for these Approach maneuvers and DSM-2 are shown in Table 3. Each of the ME burns (AAM-1 and AAM-2) included a 30-sec fuel settling burn on the TCM thrusters. Performance for each maneuver completed thus far has exceeded expectations, especially the large ME maneuvers. The last three maneuvers of this mission phase—AAM-3a, AAM-4, and M0P—are of additional significance because they used the ACS thruster set; most of the maneuvers during proximity operations will be executed on the ACS thrusters, and these initial outcomes suggest that performance will be much better than previously assumed.[13]

Approach maneuver delivery performance is summarized in Table 4. AAM-3 showed larger errors because it was decomposed into two burn segments, as discussed earlier. Delivery errors after both of the ACS maneuvers, especially AAM-3a, were very low and will be used to update modeling of the spacecraft thruster performance to reduce expected errors later in the mission.

Table 4: OSIRIS-REx Approach maneuver delivery performance.

Maneuver	Radial Error (km)	Latitude Error (deg)	Longitude Error (deg)
AAM-1	35.01	1.65	-1.70
AAM-2	-28.89	1.20	6.91
AAM-2a	N/A	N/A	N/A
AAM-3	-26.75	-1.79	10.08
AAM-3a	0.78	0.01	0.18
AAM-4	0.49	0.21	6.37
M0P	-0.13	0.18	-0.45

CONCLUSIONS

This paper describes the trajectory design, navigation conops, and key navigation results from the Approach phase of the OSIRIS-REx mission. Between August and December 2018, we acquired the first optical observations of Bennu and used them for navigation. Optical navigation performance, using three different OSIRIS-REx imagers over a wide range of distances and observing geometries, has far exceeded the 1-pixel residual error requirement throughout Approach. We performed detailed modeling and characterization of solar radiation pressure, thermal re-radiation, and telecom system performance. In part because of these modeling efforts, errors in the predicted spacecraft ephemeris used for onboard spacecraft targeting have been well below 1-sigma uncertainties from pre-encounter analysis. Between October 1 and December 2, we conducted a series of maneuvers with the ME, TCM, and ACS thruster sets to slow the OSIRIS-REx approach to Bennu and achieve rendezvous on December 3, 2018. These maneuvers had tight delivery tolerances to achieve desired scientific observation constraints for the initial characterization of Bennu. Fortunately, maneuver execution error performance has also exceeded expectations across all three sets of thrusters used during Approach.

The early observations of Bennu have revealed a fascinating world that is ripe for further exploration, and have retired some of the large modeling uncertainties that were in play before the encounter. The mosaic image of asteroid Bennu (inset) is composed of 12 PolyCam images collected on December 2 from a range of 15 miles (24 km). The mosaic was obtained at a 50° phase angle between the spacecraft, the asteroid, and the Sun, and in it, Bennu spans ~1,500 pixels. The ultimate objective of the mission is to navigate the spacecraft into contact with the surface to collect a sample and return it to Earth. With arrival at Bennu on December 3, we now transition to conducting a series of close flybys of Bennu, with the first orbit insertion successfully executed on December 31. With updated information on spacecraft performance and Bennu's physical properties in hand, we can now revisit analysis of the more challenging flight operations required to achieve the detailed surveying, global mapping, and sample collection objectives.

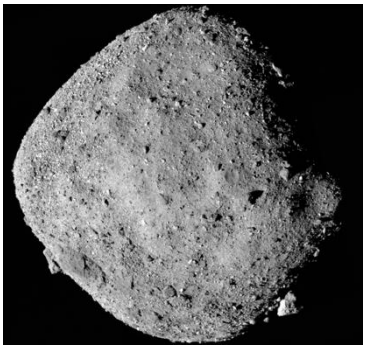

ACKNOWLEDGMENTS

The authors acknowledge members of the OSIRIS-REx team who have contributed to accomplishments described in this paper: navigation team members Ben Ashman, Kevin Berry, Michael Corvin, Andrew Liounis, Josh Lyzhoft, Jeffrey Small, Brian Sutter, and Jason Swenson; the Lockheed Martin flight operations team with special emphasis on thermal analysis data provided by Chris May and support from Javier Cerna and the telecom team; the Altimetry Working Group for early shape model deliveries used in optical navigation processing; and members of the Science Planning and Science Operations teams at the University of Arizona who have supported optical navigation observation planning.

This work is supported by NASA under Contracts NNM10AA11C, NNG12FD66C, and NNG13FC02C. OSIRIS-REx is the third mission in NASA's New Frontiers Program. Dante Lauretta of the University of Arizona, Tucson, is the principal investigator, and the University of Arizona also leads the science team and the science observation planning and data processing. Lockheed Martin Space Systems in Denver built the spacecraft and is providing flight operations. Goddard Space Flight Center and KinetX Aerospace are responsible for navigating the OSIRIS-REx spacecraft.

REFERENCES

[1] D. S. Lauretta et al., "OSIRIS-REx: Sample return from asteroid (101955) Bennu," *Space Science Reviews*, Vol. 21, 2017, pp. 925–984.

[2] D. S. Lauretta et al., "The OSIRIS-REx target asteroid (101955) Bennu: Constraints on its physical, geological, and dynamical nature from astronomical observations," *Meteoritics & Planetary Science*, Vol. 50, 2015, pp. 834–849.

[3] P. Antreasian, J. Leonard, J. McAdams, M. Moreau, B. Page, D. Wibben, and K. Williams, "OSIRIS-REx Navigation Performance During First Leg of Outbound Cruise," *41st Annual AAS Guidance, Navigation and Control Conference*, February 2018.

[4] B. Rizk et al., "OCAMS: the OSIRIS-REx camera suite." *Space Science Reviews* 214, 2018, 26.

[5] B. J. Bos et al., "Touch and Go Camera System (TAGCAMS) for the OSIRIS-REx asteroid sample return mission." *Space Science Reviews* 214, 2018, 37.

[6] C. D. Jackman and P. J. Dumont, "Optical Navigation Capabilities for Deep Space Missions," *Proceedings of the AAS/AIAA Space Flight Mechanics Meeting*, February 2013.

[7] C. D. Jackman, D. S. Nelson, L. K. McCarthy, T. J. Finley, A. J. Liounis, K. M. Getzandanner, P. G. Antreasian, and M. C. Moreau, "Optical Navigation Concept of Operations for the OSIRIS-REx Mission," *Proceedings of the AAS/AIAA Space Flight Mechanics Meeting*, February 2017.

[8] C. D. Jackman, D. S. Nelson, W. M. Owen, Jr, M. W. Buie‡, S. A. Stern, H. A. Weaver, L. A. Young, K Ennico, and C. B. Olkin, "New Horizons Optical Navigation on Approach to Pluto," 39th Annual AAS Guidance, Navigation and Control Conference, February 2016.

[9] M. C. Nolan, C. Magri, E. S. Howell, L. A. M. Benner, J. D. Giorgini, C. W. Hergenrother, R. S. Hudson, D. S. Lauretta, J.-L. Margot, S. J. Ostro, and D. J. Scheeres, "Shape model and surface properties of the OSIRIS-REx target Asteroid (101955) Bennu from radar and lightcurve observations," *Icarus*, Vol. 226, 2013, pp. 629–640.

[10] C. Hergenrother et al., "The Design Reference Asteroid for the OSIRIS-REx Mission Target (101955) Bennu," Tech. Rep. Revision 9, arXiv:1409.4704, 16 September 2014.

[11] C. Hergenrother et al., "The Design Reference Asteroid for the OSIRIS-REx Mission Target (101955) Bennu," Tech. Rep. Revision 10, Internal OSIRIS-REx Document, December 2014.

[12] O. S. Barnouin, O. S., et al., "The Shape of Bennu." AGU Fall Meeting, December 2018, Washington, DC, Abstract #P33C-3835.

[13] B. Williams, P. Antreasian, E. Carranza, C. Jackman, J. Leonard, D. Nelson, B. Page, D. Stanbridge, D. Wibben, K. Williams, et al., "OSIRIS-REx flight dynamics and navigation design," *Space Science Reviews*, Vol. 214, 2018, p. 69.

[14] D. R. Golish, et al., "OSIRIS-REx Camera Suite (OCAMS) Observations of the Earth and Its Moon During Earth Gravity Assist," *Lunar and Planetary Science Conference* 49, 2018.

[15] C. W. Hergenrother et al., "A Search for Earth Trojan Asteroids with the OSIRIS-REx Spacecraft," *Lunar and Planetary Science Conference* 48, 2017.

[16] J. M. Leonard, P. G. Antreasian, C. D. Jackman, B. Page, D. R. Wibben, and M. C. Moreau, "Orbit Determination Strategy and Simulation Performance for OSIRIS-REx Proximity Operations," *GNC 2017: 10th International ESA Conference on Guidance, Navigation & Control Systems*, May 29–June 2 2017.

[17] D. Brouwer and G. M. Clemence, *Methods of Celestial Mechanics*, Elsevier, 2013.

[18] W. M. Folkner, J. G. Williams, D. H. Boggs, R. S. Park, and P. Kuchynka, "The planetary and lunar ephemerides DE430 and DE431," *Interplanet. Netw. Prog. Rep.*, Vol. 196, 2014, pp. 1–81.

[19] D. Farnocchia and S. R. Chesley, "Asteroid 101955 (1999 RQ36) Ephemeris Delivery, JPL Solution 76," Tech. Rep., ftp://ssd.jpl.nasa.gov/pub/eph/small_bodies/orex/asteroid/IOM_343R-13-001.pdf, Feb 5, 2013.

[20] D. Farnocchia, Y. Takahashi, S. R. Chesley, R. S. Park, N. Mastrodemos, B. M. Kennedy, and B. P. Rush, "Asteroid 101955 Bennu Ephemeris Delivery, JPL Solution 103," Tech. Rep., ftp://ssd.jpl.nasa.gov/pub/eph/small_bodies/orex/asteroid/IOM_392R-18-005.pdf, November 2018.

[21] P. Antreasian, M. Moreau, C. Jackman, K. Williams, B. Page, and J. Leonard, "OSIRIS-REx orbit determination covariance studies at Bennu," *39th Annual AAS Guidance, Navigation and Control Conference*, February 2016.